Spin squeezing as an indicator of quantum chaos in the Dicke model

Lijun Song,[1] Dong Yan,[1] Jian Ma,[2] and Xiaoguang Wang[2]
[1]*Institute of Applied Physics, School of Science, Changchun University, Changchun 130022, People's Republic of China*
[2]*Department of Physics, Zhejiang Institute of Modern Physics, Zhejiang University, Hangzhou 310027, People's Republic of China*
(Received 8 November 2008; published 29 April 2009)

We study spin squeezing, an intrinsic quantum property, in the Dicke model without the rotating-wave approximation. We show that the spin squeezing can reveal the underlying chaotic and regular structures in phase space given by a Poincaré section, namely, it acts as an indicator of quantum chaos. Spin squeezing vanishes after a very short time for an initial coherent state centered in a chaotic region, whereas it persists over a longer time for the coherent state centered in a regular region of the phase space. We also study the distribution of the mean spin directions when quantum dynamics takes place. Finally, we discuss relations among spin squeezing, bosonic quadrature squeezing, and two-qubit entanglement in the dynamical processes.

DOI: 10.1103/PhysRevE.79.046220 PACS number(s): 05.45.Mt, 03.65.Ud, 42.50.Dv

I. INTRODUCTION

Chaos plays a key role in studying the boundary between the classical and quantum worlds not only because of the importance of chaos in classical physics [1] but also because there is no direct analog of chaos in quantum mechanics. Then, it is natural to study the quantum properties of a Hamiltonian, of which the classical analog is nonintegrable and therefore displays chaotic dynamic behaviors [2]. Various signatures of quantum chaos have been identified, such as the spectral properties of the generating Hamiltonian [3], phase-space scarring [4], hypersensitivity to perturbation [5], and fidelity decay [6–9], which indicate an underlying chaotic presence in the corresponding quantum dynamics. Recently, the entanglement has been identified as another signature of quantum chaos [10–18]. The entanglement inherent in quantum-chaotic systems can provide a valuable approach to quantum chaos.

Entanglement and squeezing are two typical purely quantum effects. Interestingly, it was found that spin squeezing [19–23] is closely related to and implies quantum entanglement [21]. To be more exact, if a spin state with a certain parity is spin squeezed according to the definition from Kitagawa and Ueda [19], a quantitative relation is obtained between the spin squeezing parameter and the concurrence [24], which quantifies the entanglement of two spin-half particles [25,26]. The close relationship between the entanglement and spin squeezing, as well as the entanglement as a signature of quantum chaos, motivate us to explore the role of spin squeezing in quantum-chaotic spin systems. The relations between light squeezing and quantum chaos have been studied [27], however, relations between spin squeezing and quantum chaos were less addressed [28].

The quantum-chaotic properties [29] of the Dicke model (DM) without rotating-wave approximation (RWA) [30] have been extensively studied, and spin squeezing has also been investigated very recently [31,32] but without being connected with the chaos. In this work, we consider the quantum DM [33–38], an interaction model of the radiation field with a collection of two level atoms, which exhibits chaos without RWA. The phase space of the DM is finite, and the Poincaré section of the phase space is compact which allows analysis of quantum and classical dynamics and facilitates the study of the role of spin squeezing in the system. There are several definitions of spin squeezing in the literature [19–22]. Typically, there are two types of spin squeezing defined in spin-j systems from Kitagawa *et al.* [19] and Wineland *et al.* [20], where $j=N/2$ and N is the number of atoms. In our study, we use the first definition quantified by the following spin squeezing parameter:

$$\xi^2 = \frac{2(\Delta J_{\vec{n}_\perp})^2}{j} = \frac{4(\Delta J_{\vec{n}_\perp})^2}{N}, \tag{1}$$

where the subscript $\vec{n}_\perp$ refers to an axis perpendicular to the mean spin direction (MSD) $\vec{n}_1=\langle\vec{J}\rangle/|\langle\vec{J}\rangle|$, in which the variance $(\Delta J)^2$ is minimal, and $J_{\vec{n}_\perp}=\vec{J}\cdot\vec{n}_\perp$. The inequality $\xi^2<1$ indicates that the system is spin squeezed.

We study the dynamical behaviors of the spin squeezing quantified by ξ^2 for specific initial states. In the DM, we show that the spin squeezing disappears after a very short time for an initial coherent state (CS) centered in a chaotic region, while it persists over a longer time for the initial CS centered in a regular region of the classical phase space. In other words, the spin squeezing can reveal the chaotic and regular structures in phase space.

The paper is organized as follows. In Sec. II, we introduce the DM and its corresponding classical Hamiltonian. In Sec. III, we study in detail dynamical evolutions of spin squeezing parameter and examine distributions of MSDs during the quantum dynamics. The spin squeezing vanishing time is introduced in order to characterize spin squeezing and study classical-quantum correspondence. We make comparisons among the dynamics of the spin squeezing, bosonic quadrature squeezing, and two-qubit quantum entanglement. The conclusions are given in Sec. IV.

II. DICKE MODEL

The DM describes the dipole interaction of N two-level atoms with n bosonic field modes. Here we shall only consider the single-mode radiation field case with $n=1$. A standard approach to such quantum-optics Hamiltonian is to make the RWA, rendering the model integrable. We do not

make the RWA here, so the DM Hamiltonian is written as ($\hbar=1$ hereafter)

$$H=\omega J_z+\omega_0 a^\dagger a+\frac{R}{\sqrt{2j}}(J_+a+J_-a^\dagger)+\frac{R'}{\sqrt{2j}}(J_+a^\dagger+J_-a), \tag{2}$$

where ω and ω_0 are frequencies associated with free Hamiltonians for atoms and field, respectively. R and R' are the coupling parameters. The usual RWA is recovered by setting $R'=0$. The field observables are described by means of the creation and annihilation operators a and $a^\dagger$, j is the length of the collective spin operators, J_z is the operator of the atomic inversion, and $J_\pm$ are the collective atomic pseudospin operators. They satisfy the SU(2) Lie algebra,

$$[J_+,J_-]=2J_z,\quad [J_z,J_\pm]=\pm J_\pm. \tag{3}$$

The Hilbert space of this algebra is spanned by the Dicke states $|j,m\rangle(m=-j,-j+1,\ldots,j-1,j)$, which are the eigenstates of J^2 and J_z with the eigenvalues $j(j+1)$ and m. The pseudospin operators act on these states as $J_\pm|j,m\rangle=\sqrt{j(j+1)-m(m\pm1)}|j,m\pm1\rangle$. This model is used to describe both cavity quantum electrodynamics (QED) experiments [39,40] and trapped-ion systems, where interactions with different couplings $R\neq R'$ can be obtained [41,42].

In our case, we take the initial states to be CS, namely, minimum uncertainty wave packets centered in the corresponding classical phase spaces, which allows us to explore the relation between the spin squeezing and classical chaos. The initial quantum states chosen in the present study are as follows:

$$|\psi(0)\rangle=|\mu\rangle\otimes|\nu\rangle\equiv|\mu\nu\rangle, \tag{4}$$

where $|\mu\nu\rangle$ is a product of the atomic and field CS defined as [43]

$$|\mu\rangle=(1+\mu\mu^*)^{-j}e^{\mu J_+}|j,-j\rangle, \tag{5}$$

$$|\nu\rangle=e^{-\nu\nu^*/2}e^{\nu a^\dagger}|0\rangle. \tag{6}$$

Here $j=N/2$ and $|0\rangle$ is the bosonic field ground state. The variables μ and ν can be written as a function of the classical variables in the corresponding phase spaces [44],

$$\mu=\frac{p_1+iq_1}{\sqrt{4j-(p_1^2+q_1^2)}}, \tag{7}$$

$$\nu=\frac{1}{\sqrt{2}}(p_2+iq_2), \tag{8}$$

where q_1,p_1,q_2,p_2 describe the phase space of the system under consideration with indices 1 and 2 for the atomic and field subsystems, respectively. For spin coherent state $|\mu\rangle$, the mean atom number $\langle\mathcal{N}\rangle=\langle j+J_z\rangle$ is proportional to the quantity $|\mu|^2$ [45]. This state can be regarded as a binomial state which comes from the fact that their atom distribution is simply a binomial distribution, and the absolute value $|\mu|$ normally ranges between 0 and 1 [46]. For the bosonic coherent state $|\nu\rangle$, $|\nu|^2$ represents the mean photon number, which ranges from 0 to ∞ in principle. The phases of μ and ν is from 0 to 2π.

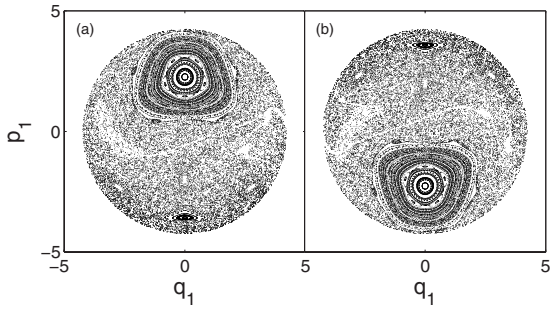

FIG. 1. The Poincaré section for the spin degree of freedom in the resonant case ($\omega=\omega_0=1$), energy $E=8.5$, and $j=4.5$ in a nonintegrable case ($R=0.5$ and $R'=0.2$). (a) Section with $q_2=0.0$ and $p_2>0.0$; (b) Section with $q_2=0.0$ and $p_2<0.0$.

The classical Hamiltonian corresponding to Eq. (2) can be obtained by a standard procedure as [43,47]

$$\begin{aligned}\mathcal{H}(q_1,p_1,q_2,p_2)&=\langle\mu\nu|H|\mu\nu\rangle\\&=\frac{\omega}{2}(p_1^2+q_1^2-2j)+\frac{\omega_0}{2}(p_2^2+q_2^2)\\&\quad+\frac{\sqrt{4j-(p_1^2+q_1^2)}}{4j}(R_+p_1p_2+R_-q_1q_2),\end{aligned} \tag{9}$$

with $R_\pm=R\pm R'$.

The classical dynamics associated with this Hamiltonian were explored before [44]. It is shown that the integrable situations are recovered when either R or R' is zero. Our aim is to investigate the time evolution of the initially quasiclassical wave packet along with the occurrence of atomic spin squeezing. Particularly, we are looking for the possible differences in the wave-packet dynamics when we compare the case of an initial quantum state centered in a chaotic region and one in a regular region of the classical phase space. The connection with the classical dynamics is established by choosing CSs as initial states centered at the corresponding points of the phase space. Then, we let the system evolve by means of Hamiltonian (2) and explore the spin squeezing dynamics by solving numerically the Schrödinger equation. In Fig. 1, we show the Poincaré section of the classical counterpart for the spin degree of freedom defined by the section $q_2=0$ in the four-dimensional phase space so that every time a trajectory pierces this section with $p_2>0$ or $p_2<0$ the corresponding point (q_1, p_1) is plotted. Here, the total energy is fixed at $E=8.5$, $j=9/2$, and $\omega=\omega_0=1$. The limit of atomic phase space is indicated by a border at radius equal to $\sqrt{4j}$. In the plot, we choose the coupling parameters $R=0.5$ and $R'=0.2$, which yields a mixture of regular and chaotic areas of a significant size. Fixed points and near-periodic orbits surrounded by the chaotic sea are evident.

Here, we choose a relatively lower value of $j=9/2$. Our aim is to study the corresponding relations between spin squeezing and the classical chaotic dynamics, and the classical limit means that the value of particle number N ap-

proaches infinity, while the spin squeezing, a typical purely quantum effects, requests a lower value of $j=N/2$, which ensures manifestation of quantum properties. So, an intermediate value of j is needed. We have checked the values of $j=17/2,21/2,50/2$ and found that the results of spin squeezing were qualitatively the same as the case of $j=9/2$. Moreover, in order to compare our results with those on relations between linear entropy and chaos in Ref. [11], the value $j=9/2$ is chosen.

III. DYNAMICS OF SPIN SQUEEZING

Now, we study dynamics of spin squeezing and first consider the MSDs. It will be found that the MSDs display interesting behaviors due to the presence of quantum chaos.

A. Mean spin directions

According to the definitions of spin squeezing, we first need to know the MSDs determined by expectation values $\langle J_\alpha \rangle$ with $\alpha \in \{x,y,z\}$. The mean spin direction $\vec{n}_1$ can be written in the spherical coordinate as

$$\vec{n}_1 = (\sin\theta\cos\phi, \sin\theta\sin\phi, \cos\theta), \tag{10}$$

where θ and ϕ are the polar angle and azimuthal angle, respectively. The angles θ and ϕ are given by

$$\theta = \arccos\left(\frac{\langle J_z\rangle}{|\vec{J}|}\right),$$

$$\phi = \begin{cases} \arccos\left(\dfrac{\langle J_x\rangle}{|\vec{J}|\sin(\theta)}\right) & \text{if} \quad \langle J_y\rangle > 0 \\ 2\pi - \arccos\left(\dfrac{\langle J_x\rangle}{|\vec{J}|\sin(\theta)}\right) & \text{if} \quad \langle J_y\rangle \le 0, \end{cases} \tag{11}$$

where $|\vec{J}| = \sqrt{\langle J_x\rangle^2 + \langle J_y\rangle^2 + \langle J_z\rangle^2}$ is the magnitude of the mean spin. Here we also give the following two directions: $\vec{n}_2 = (-\sin\phi, \cos\phi, 0)$ and $\vec{n}_3 = (-\cos\theta\cos\phi, -\cos\theta\sin\phi, \sin\theta)$, both perpendicular to $\vec{n}_1$. The above expressions are valid for $\theta \neq 0, \pi$. For $\theta = 0, \pi$, the mean spin is along the $\pm z$ direction, and the possible choices of ϕ can be $\phi = 0, \pi$.

We study quantum dynamics with initial states in different regions of the phase space—chaotic, regular, and intermediate from the regular to the chaotic. For convenience, we fix $q_1=0$ and vary p_1 in Fig. 1(a). This line on the section includes all these regions we are exploring. For the regular regions, we choose two representative points $p_1=2.0$ and $p_1=-3.5$; for the chaotic regions, we choose $p_1=0$ and $p_1=-1.0$; and for the intermediate regions, we choose $p_1=1.5$ and $p_1=-1.5$.

In Fig. 2, we plot the MSDs for different initial states with a fixed $q_1=0$ and different p_1. We observe that the MSDs are localized in a fixed region for initial states centered in a regular region. For $p_1=2.0$, the fixed region is approximately limited to $\frac{\pi}{2} \le \theta \le \frac{3\pi}{4}$. When the initial state is centered in the chaotic region $p_1=0$, the MSDs are randomly over the whole range of θ and ϕ. The case of $p_1=1.5$ displays the intermediate behaviors, with the MSDs localized in a finite region

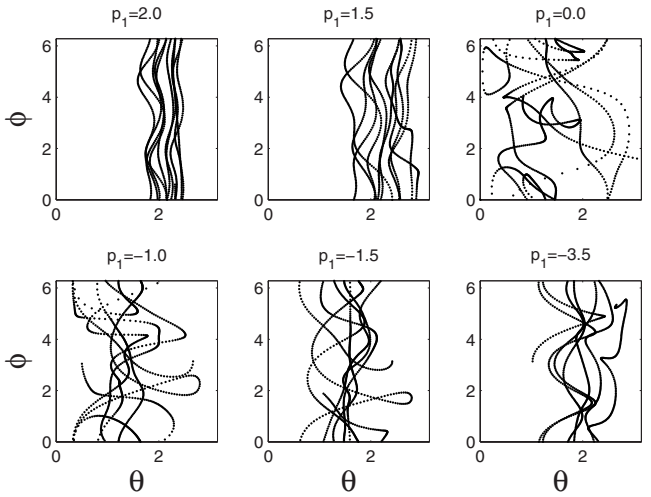

FIG. 2. Distributions of the mean spin directions for initial states with $q_1=0$ and different p_1 in Fig. 1(a). Parameters $E=8.5, j=4.5, q_2=0, p_2>0$.

$\frac{\pi}{2} \le \theta \le \pi$, which is larger than that of the above case of the regular region. With $p_1=-1.0$, $p_1=-1.5$, and $p_1=-3.5$, the MSDs exhibit similar behaviors. Then, from the MSDs, we can qualitatively get some information on the presence of chaos in the system.

B. Spin squeezing

Having known the MSDs, in order to compute the squeezing parameter, we need to know the following minimal variance [26]:

$$(\Delta J_{\vec{n}_\perp})^2 = \langle J_{\vec{n}_\perp}^2\rangle = \frac{1}{2}\langle J_{\vec{n}_2}^2 + J_{\vec{n}_3}^2\rangle - \frac{1}{2}\sqrt{(\langle J_{\vec{n}_2}^2 - J_{\vec{n}_3}^2\rangle)^2 + \langle [J_{\vec{n}_2}, J_{\vec{n}_3}]_+\rangle^2}, \tag{12}$$

with

$$J_{\vec{n}_2} = -J_x\sin\phi + J_y\cos\phi,$$

$$J_{\vec{n}_3} = -J_x\cos\theta\cos\phi - J_y\cos\theta\sin\phi + J_z\sin\theta. \tag{13}$$

Then, we can numerically calculate the spin squeezing.

We choose two fixed points at $q_1=0$, $p_1=2.0$ and $q_1=0$, $p_1=-3.5$, which are in the regular regions, and another two points $q_1=0$, $p_1=0$ and $q_1=0$, $p_1=-1.0$ well in the chaotic sea, and the numerical results of spin squeezing parameter ξ^2 are shown in Fig. 3. For initial states in the regular region [see Fig. 3(a)], as the dynamics evolves, the spin squeezing persists over a relatively longer time ($t \approx 9.0$), whereas the spin squeezing vanishes for states in the chaotic region [see Fig. 3(b)] after a very short time ($t \approx 1.8$).

From the above plots, we observe that the spin squeezing vanishes at some time after which no squeezing occurs. It will be convenient to define a spin squeezing vanishing time t_v, which characterizes how long the spin squeezing survives. By numerical calculations, we find that the vanishing time is

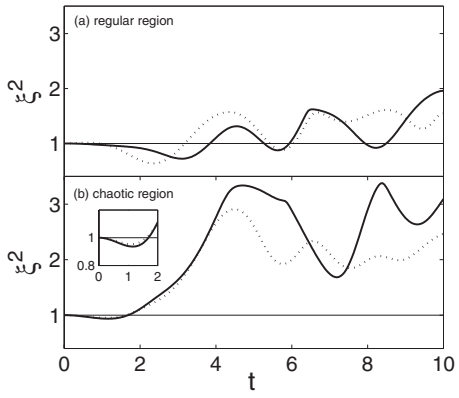

FIG. 3. Dynamical evolution of the spin squeezing parameter ξ^2 for the initial states with $q_1=0$ and different p_1. (a) Regular region corresponding to Fig. 1(a): $p_1=2.0$ (solid line) and $p_1=-3.5$ (dashed line); (b) Chaotic region corresponding to Fig. 1(a): $p_1=0$ (solid line) and $p_1=-1.0$ (dashed line).

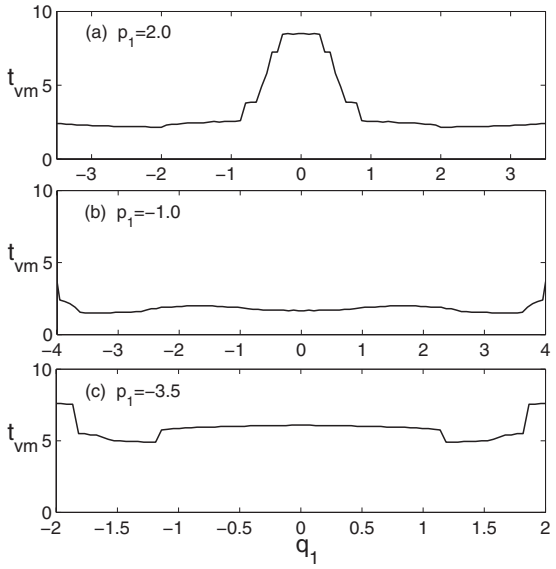

FIG. 4. Average spin squeezing vanish time t_{vm} versus q_1, corresponding to the straight line at $p_1=2.0,-1.0,-3.5$ in the Poincaré sections in Fig. 1(a). The other parameters $E=8.5$ and $j=4.5$.

not symmetric as a function of q_1 at a fixed p_1, which is contrary to our expectations from Fig. 1(a). In other words, there is no good classical-quantum correspondence. To solve this problem, we find that in fact we need the Poincaré sections for both $p_2>0$ and $p_2<0$, which become complete in the phase space. Then, for a point with same chaotic property, there will be two corresponding points (for the case of $q_1\neq 0$) in Figs. 1(a) and 1(b), respectively. This is a key observation, from which we know that there are two initial coherent states correspond to one classical point in phase space. One-to-many correspondence often happens between classical and quantum mechanics. For instance, two different quantum Hamiltonians may correspond to one classical Hamiltonian due to the commuting of two classical variables. Thus, we may define average vanishing time $t_{vm}=1/2[t_v(p_2>0)+t_v(p_2<0)]$ and plot t_{vm} versus q_1 at a fixed p_1.

As seen from Fig. 4 (note that the ranges of q_1 are different in different subfigures), we find that the vanishing time is ideally symmetric with respect to q_1. From Fig. 4(a) ($p_1=2.0$), a bump region of longer vanishing time is evident, which corresponds to the big regular island in Fig. 1(a). When $p_2=-1.0$, in classical phase space, this line belongs to chaotic region, so the squeezing vanishing time should be small, which is just what we observed in Fig. 4(b). Here, the vanishing time is small and displays a flat line. When $p_1=-3.5$, the line crosses a small regular island. We see a flat region with relatively longer vanishing time in the middle of Fig. 4(c), which corresponds to the small island. From the above analysis, we have found a good classical-quantum correspondence via the study of spin squeezing vanishing time.

We see that the underlying classical chaos indeed controls the quantum dynamics of spin squeezing in the DM. The spin squeezing is *very sensitive* to the classical chaos, and the classical chaos suppresses the spin squeezing. In contrast, the classical chaos enhances the bipartite entanglement quantified by the linear entropy in the DM [11]. So, the underlying classical chaos has different effect on the two typical purely quantum-mechanical phenomena; the spin squeezing and the bipartite entanglement.

C. Relations of spin squeezing, bosonic quadrature squeezing, and entanglement

In this section, we will first compare dynamical behaviors between spin squeezing and bosonic quadrature squeezing, and then study the relations between spin squeezing and pairwise entanglement.

1. Comparison of spin squeezing and bosonic quadrature squeezing

Here, we review bosonic quadrature squeezing. There is a definition of ζ^2 as a bosonic squeezing parameter, which provides an atomic squeezing counterpart to determine whether a state is squeezed. The parameter is given by [48]

$$\zeta^2=\min_{\theta\in[0,2\pi)}(\Delta X_\theta)^2, \tag{14}$$

where

$$X_\theta=X\cos\theta+P\sin\theta=ae^{-i\theta}+a^\dagger e^{i\theta} \tag{15}$$

with $X=X_0$ and $P=X_{\pi/2}$ being special cases. So, the minimum value of $(\Delta X_\theta)^2$ with respect to θ, and $\zeta^2<1$ indicates the so-called principle squeezing. And the two quadrature operators X and P are given by

$$X=a+a^\dagger,\quad P=-i(a-a^\dagger), \tag{16}$$

where a and $a^\dagger$ are the annihilation and creation operators of a boson, respectively. For a quantum state, from Eq. (14), we obtain

$$\zeta^2=1+2\langle a^\dagger a\rangle-2|\langle a\rangle|^2-2|\langle a^2\rangle-\langle a\rangle^2|.$$

Having understood the notions of the bosonic quadrature squeezing, we compare the dynamical behaviors of the two types of squeezing. In Fig. 5(b), we show that the bosonic quadrature squeezing (dashed line) disappears after a very short time for an initial CS centered in a chaotic region and

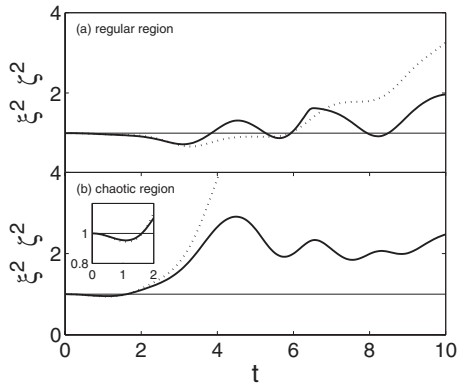

FIG. 5. Parameters ξ^2 (solid line) and ζ^2 (dashed line) versus time. The other parameters $E=8.5$ and $j=4.5$ and (a) $q_1=0$ and $p_1=2.0$; (b) $q_1=0$ and $p_1=-1.0$.

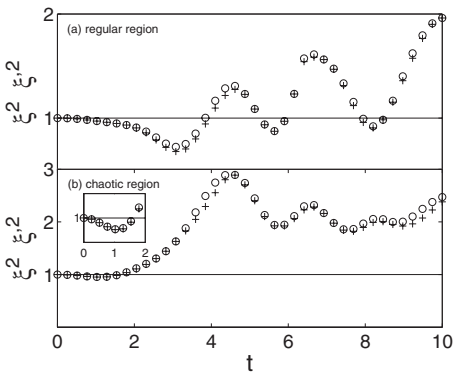

FIG. 6. Parameters ξ^2 (circle points) and ξ'^2 (cross) versus time. The other parameters $E=8.5$ and $j=4.5$ and (a) $q_1=0$ and $p_1=2.0$; (b) $q_1=0$ and $p_1=-1.0$.

the spin squeezing disappears as well, while the two squeezings persist over a longer time for the CS centered in a regular region of the classical phase space [see Fig. 5(a)]. In other words, both spin squeezing and bosonic quadrature squeezing can reveal the chaotic and regular structures in phase space.

We also notice that the two squeezing parameters are nearly but not completely identical for low time t. One reason for this behavior is that the two parameters are connected, namely, the spin squeezing parameter reduces to the bosonic one in the limit of large number of atoms N and low excitations [49]. Another reason is that they all start from one. Also, the initial spin coherent state reduces to the bosonic coherent state, and the Hamiltonian reduces to the two-boson Hamiltonian under the same limit. As we choose $\omega_0=\omega$, the Hamiltonian is symmetric under swapping of two bosons. However, for larger t, these two parameters become different due to the complexity of interactions between spins and bosons in the Dicke model.

2. Comparison of spin squeezing and entanglement

The DM describes a collection of N two-level atoms interacting with a single-mode radiation field. Given the N-qubit system, we can study entanglement of a pair of qubits (say qubits 1 and 2) by tracing out other $N-2$ qubits. Entanglement for the two-qubit mixed state $\rho_{12}=\mathrm{Tr}_{3,\ldots,N}(\rho)$ can be quantified by the concurrence [24]. The concurrence is defined as

$$C=\lambda_1-\lambda_2-\lambda_3-\lambda_4, \tag{17}$$

with the quantities λ_i being the square roots of the eigenvalues in nonascending order of the matrix product $\rho_{12}(\sigma_{1y}\otimes\sigma_{2y})\rho_{12}^{*}(\sigma_{1y}\otimes\sigma_{2y})$. ρ_{12}^{*} denotes the complex conjugate of ρ_{12}. Here, we remove the max function in the usual definition of the concurrence, namely, $C\leq 0$ implies no entanglement.

In Ref. [17], it is found that the concurrence is suppressed by chaos in the quantum kicked top model. We will see that the same conclusion holds for our Dicke model. It was known that spin squeezing is closely related to entanglement [21], and if a state with parity is spin squeezed, the following relation between the squeezing parameter ξ^2 and the concurrence [24] C is obtained [26]: $\xi^2=1-(N-1)C$. One should note two conditions for this equality to hold. One is that the spin states must have a fixed parity, and the other is that it must be a spin-squeezed state. If a state is not spin squeezed, we cannot get this relation. For our state vector at time t, usually there is no fixed parity, so we cannot get the simple relation between the spin squeezing parameter ξ^2 and C. In order to make a comparison between spin squeezing and pairwise entanglement, it is convenient to define the following quantity:

$$\xi'^2=1-(N-1)C, \tag{18}$$

and see whether the parameter ξ'^2 coincides with ξ^2. If we use ξ'^2 to characterize the pairwise entanglement, it is clear that if $\xi'^2<1$ ($\xi'^2\geq 1$), the state is entangled (not entangled).

The numerical results of ξ^2 and ξ'^2 versus time are given in Fig. 6. In Fig. 6(a), initially, $\xi^2=\xi'^2=1$ since there exists no spin squeezing and no entanglement. As dynamics takes place, ξ^2 and ξ'^2 do not always coincide with each other for the regular regions. Especially, between $t=3$ and $t=4$, there is a clear difference between them. However, in the squeezing area the two parameters coincide very well for the chaotic case in Fig. 6(b), which indicates that the relation between the squeezing parameter and the concurrence holds, namely, $\xi^2=1-(N-1)C$. In other words, the excellent agreement between ξ^2 and ξ'^2 implies that the spin state may display a parity symmetry. The numerical results also show that the agreement is good when we choose different initial states.

IV. CONCLUSIONS

We have studied the spin squeezing in the DM whose Hamiltonian dynamics is chaotic in the classical limit and found that the underlying chaotic motion greatly affects the spin squeezing properties. Spin squeezing vanishes after a very short time for an initial CS centered in a chaotic region of the phase space, whereas the spin squeezing persists over a longer time for the CS centered in a regular region. Manifestation of chaotic motion is found in the MSDs, which expand over a large area when chaos is present.

As the spin squeezing eventually vanishes in this model, we have defined the squeezing vanishing time to characterize

the squeezing properties. We have found a good classical-quantum correspondence via the studies of the vanishing time. We also studied relations among behaviors of spin squeezing, bosonic quadrature squeezing, and the pairwise entanglement. The bosonic quadrature squeezing displays similar behaviors, and close relationship was found between the pairwise entanglement and spin squeezing.

The spin squeezing is very sensitive to the underlying chaos. This means that it is a good indicator of quantum chaos in the DM model. An adequate way of investigating the problem of quantum chaos is by studying the dynamics of intrinsically quantum properties [11]. Spin squeezing is an important purely quantum-mechanical effect, and here we have highlighted the connection between spin squeezing and quantum chaos.

ACKNOWLEDGMENTS

This work was supported by NSFC under Grant No. 10874151, NFRPC under Grant No. 2006CB921205, and Program for New Century Excellent Talents in University (NCET).

[1] R. C. Hilborn, *Chaos and Nonlinear Dynamics* (Oxford University Press, Oxford, 2000).
[2] M. C. Gutzwiller, *Chaos in Classical and Quantum Mechanics* (Springer, Berlin, 2001).
[3] F. Haake, *Quantum Signature of Chaos* (Springer-Verlag, Berlin, 1991).
[4] E. J. Heller, Phys. Rev. Lett. **53**, 1515 (1984).
[5] R. Schack, G. M. D'Ariano, and C. M. Caves, Phys. Rev. E **50**, 972 (1994).
[6] A. Peres, Phys. Rev. A **30**, 1610 (1984); J. Emerson, Y. S. Weinstein, S. Lloyd, and D. G. Cory, Phys. Rev. Lett. **89**, 284102 (2002).
[7] Y. S. Weinstein and C. S. Hellberg, Phys. Rev. E **71**, 016209 (2005); Y. S. Weinstein and C. S. Hellberg, *ibid.* **71**, 035203(R) (2005).
[8] T. Gorin, T. Prosen, T. H. Seligman, and M. Žnidarič, Phys. Rep. **435**, 33 (2006).
[9] R. A. Jalabert and H. M. Pastawski, Phys. Rev. Lett. **86**, 2490 (2001).
[10] Y. S. Weinstein and L. Viola, Europhys. Lett. **76**, 746 (2006).
[11] K. Furuya, M. C. Nemes, and G. Q. Pellegrino, Phys. Rev. Lett. **80**, 5524 (1998).
[12] P. A. Miller and S. Sarkar, Phys. Rev. E **60**, 1542 (1999).
[13] H. Fujisaki, T. Miyadera, and A. Tanaka, Phys. Rev. E **67**, 066201 (2003).
[14] A. J. Scott and C. M. Caves, J. Phys. A **36**, 9553 (2003).
[15] S. Bettelli and D. L. Shepelyansky, Phys. Rev. A **67**, 054303 (2003).
[16] B. Georgeot and D. L. Shepelyansky, Phys. Rev. E **62**, 6366 (2000).
[17] X. Wang, S. Ghose, B. C. Sanders, and B. Hu, Phys. Rev. E **70**, 016217 (2004).
[18] M. Novaes and M. A. M. de Aguiar, Phys. Rev. E **70**, 045201 (2004); M. Novaes, Ann. Phys. **318**, 308 (2005).
[19] M. Kitagawa and M. Ueda, Phys. Rev. A **47**, 5138 (1993).
[20] D. J. Wineland, J. J. Bollinger, W. M. Itano, and D. J. Heinzen, Phys. Rev. A **50**, 67 (1994).
[21] A. S. Sørensen, L.-M. Duan, J. I. Cirac, and P. Zoller, Nature (London) **409**, 63 (2001); A. Søndberg Sørensen, Phys. Rev. A **65**, 043610 (2002); A. S. Sørensen and K. Mølmer, Phys. Rev. Lett. **86**, 4431 (2001).
[22] H. Pu, W. Zhang, and P. Meystre, Phys. Rev. Lett. **89**, 090401 (2002); S. Raghavan, H. Pu, and N. P. Bigelow, Opt. Commun. **188**, 149 (2001).
[23] A. Kuzmich, K. Mølmer, and E. S. Polzik, Phys. Rev. Lett. **79**, 4782 (1997); J. Hald, J. L. Sørensen, C. Schori, and E. S. Polzik, *ibid.* **83**, 1319 (1999); A. Kuzmich, L. Mandel, and N. P. Bigelow, Phys. Rev. Lett. **85**, 1594 (2000); L. Vernac, M. Pinard, and E. Giacobino, Phys. Rev. A **62**, 063812 (2000).
[24] S. Hill and W. K. Wootters, Phys. Rev. Lett. **78**, 5022 (1997); W. K. Wootters, *ibid.* **80**, 2245 (1998).
[25] D. Ulam-Orgikh and M. Kitagawa, Phys. Rev. A **64**, 052106 (2001).
[26] X. Wang and B. C. Sanders, Phys. Rev. A **68**, 012101 (2003).
[27] K. N. Alekseev and D. S. Primak, JETP **86**, 61 (1998); K. N. Alekseev, Opt. Commun. **116**, 468 (1995); K. N. Alekseev and J. Perina, Phys. Rev. E **57**, 4023 (1998); K. N. Alekseev and J. Perina, Phys. Lett. A **231**, 373 (1997).
[28] L. J. Song, X. Wang, D. Yan, and Z. G. Zong, J. Phys. B **39**, 559 (2006).
[29] G. A. Finney and J. Gea-Banacloche, Phys. Rev. E **54**, 1449 (1996); C. Emary and T. Brandes, *ibid.* **90**, 044101 (2003); Phys. Rev. E **67**, 066203 (2003); X. W. Hou and B. Hu, Phys. Rev. A **69**, 042110 (2004); L. Sanz and K. Furuya, e-print arXiv:quant-ph/0507025.
[30] R. H. Dicke, Phys. Rev. **93**, 99 (1954).
[31] G. R. Jin and S. W. Kim, Phys. Rev. Lett. **99**, 170405 (2007); Phys. Rev. A **76**, 043621 (2007).
[32] M. K. Henry, J. Emerson, R. Martinez, and D. G. Cory, Phys. Rev. A **74**, 062317 (2006).
[33] F. Haake, M. Kuś, J. Mostowski, and R. Scharf, in *Coherence, cooperation and fluctuations*, edited by F. Haake, L. Narducci, and D. Walls (Cambridge University Press, Cambridge, 1986), p. 220.
[34] F. Haake, M. Kuś, and R. Scharf, Z. Phys. B: Condens. Matter **65**, 381 (1987).
[35] H. Frahm and H. J. Mikeska, Z. Phys. B: Condens. Matter **60**, 117 (1985).
[36] G. J. Milburn, e-print arXiv:quant-ph/9908037.
[37] G. M. D'Ariano, L. R. Evangelista, and M. Saraceno, Phys. Rev. A **45**, 3646 (1992).
[38] B. C. Sanders and G. J. Milburn, Z. Phys. B: Condens. Matter **77**, 497 (1989).
[39] E. Solano, G. S. Agarwal, and H. Walther, Phys. Rev. Lett. **90**, 027903 (2003).
[40] L. Davidovich, A. Maali, M. Brune, J. M. Raimond, and S. Haroche, Phys. Rev. Lett. **71**, 2360 (1993).
[41] J. I. Cirac, A. S. Parkins, R. Blatt, and P. Zoller, Adv. At.,

Mol., Opt. Phys. **37**, 237 (1996).
[42] E. Solano, R. L. de Matos Filho, and N. Zagury, Phys. Rev. Lett. **87**, 060402 (2001).
[43] W. M. Zhang, D. H. Feng, and R. Gilmore, Rev. Mod. Phys. **62**, 867 (1990).
[44] M. A. M de Aguiar, K. Furuya, C. H. Lewenkopf, and M. C. Nemes, Ann. Phys. **216**, 291 (1992); Europhys. Lett. **15**, 125 (1991).
[45] J. M. Radcliffe, J. Phys. A **4**, 313 (1971).
[46] D. Stoler, B. E. A. Saleh, and M. C. Teich, Opt. Acta (London) **32**, 345 (1985).
[47] P. Kramer and M. Saraceno, *Geometry of the Time-Dependent Variational Principle in Quantum Mechanics*, Lecture Notes in Physics Vol. 140 (Springer-Verlag, New York, 1981).
[48] A. Lukš, V. Peřinová, and Z. Hradil, Acta Phys. Pol. A **74**, 713 (1988); A. Lukš, V. Peřinová, and J. Peřina, Opt. Commun. **67**, 149 (1988); K. N. Alekseev and D. S. Pri ĭ mak, JETP **86**, 61 (1998); J. Bajer, A. Miranowicz, and R. Tanaś, Czech. J. Phys. **52**, 1313 (2002).
[49] X. Wang and B. C. Sanders, Phys. Rev. A **68**, 033821 (2003).